Proceedings of the International School and Conference on Photonics, PHOTONICA09

Optical Properties of Runaway Electron Preionized Diffuse Discharges and Their Applications for Excilamps and Lasers

V. Tarasenko*, E. Baksht, A. Burachenko, I. Kostyrya, M. Lomaev and D. Rybka

High Current Electronics Institute, Tomsk, Russia

The results of experimental investigations of diffuse (volume) nanosecond elevated-pressure discharges in a non-uniform electric field at a time resolution of a recording system being equal to ≈ 100 ps are presented in this paper. The application of the runaway electrons preionized diffuse discharge is promising for obtaining high-power radiation pulses in the VUV and UV spectral region.

PACS numbers: 52.80.Tn, 42.55.Lt, 42.60.Lh

1. Introduction

At the present time, high-pressure pulsed diffuse discharges find wide application in science and technology, in particular in designs of gas and plasma lasers. Diffuse discharges are produced using various preionization sources and discharge gaps with a homogeneous electric field. Since the late 1960s, the initiation of atmospheric-pressure diffuse discharges in various gases has been known to be possible even with no additional preionization [1, 2], for which short high-voltage pulses and discharge gaps with a cathode of small curvature radius are used. Atmospheric-pressure diffuse discharges were obtained in helium [1], in air [2], and later in SF_6 [3]. A peculiar feature of this discharge type is the generation of X-rays [1, 2] and runaway electron beams [4]. Since 1990 the interest in this field has been lost. Apparently, this is due to the subnanosecond time of the processes occurring in the REP DD gap and thus to the complexity of nanosecond and subnanosecond high-voltage pulsers and measurements of discharge and runaway e-beam characteristics. In five recent years, interest in this discharge mode has been rekindled [5–13]. It was found that atmospheric-pressure discharges in an inhomogeneous electric field feature a number of unique properties; in particular the specific input power can reach ≈ 800 MW/cm^3 at the gap center [6]. Another peculiarity of the runaway electrons preionized diffuse discharge (REP DD) is that its ignition is slightly affected by the polarity of a nanosecond voltage pulse [7]. A diffuse discharge with a voltage risetime of tens of nanoseconds was obtained in [8], and a diffuse discharge with a voltage of tens of kilovolts was realized in [6]. In the batch mode, the REP DD retained its properties at high repetition rate, e.g., up to 3 kHz [9]. However, this discharge type is still poorly understood and primarily due to the short duration of the initial discharge phase responsible for its diffuse character.

The objective of the work was to investigate the conditions and the properties of subnanosecond (up to ≈ 100 ps) and nanosecond REP DDs. In the experiments, the time resolution of a measuring system was ≈ 100 ps.

2. Experimental procedure and equipment

The discharge parameters (current–voltage characteristics, space form, and radiation spectra) were studied on RADAN-220 and SLEP-150 pulsers [10]. The inner diameter of the gas discharge chamber was ≈ 50 mm. Cathode of small curvature radius and plane anode ensured field amplification near the cathode. The cathode was either a steel sphere of diameter 9.5 mm or a steel foil tube of diameter ≈ 6 mm and thickness 100 μm. The plane anode was a brass plate connected to the chamber case with shunt. In the studies, foil and grid anodes were also used. With the foil anode, the characteristics of a supershort avalanche electron beam (SAEB) [5] were measured on the collector placed downstream of the foil. A more detailed description of studies on SAEB's can be found in [10–13]. The interelectrode gap was between 0 (short-circuit) and 19 mm. In experiments with short voltage pulse durations, the SLEP-150 nanosecond pulser was used [13]. The pulser produced voltage pulses of amplitude up to 150 kV (across a high-resistance load) with a voltage risetime of ≈ 0.3 ns. At the output of the SLEP-150 pulser, there was a transmission line. When filled with transformer oil and air, the transmission line had an impedance of 100 Ω and 140 Ω, respectively. The voltage pulse FWHM in the transmission line of the SLEP-150 pulser was variable between 1 and 0.1 ns because of a closing switch located at the input of the air-filled transmission line. In a number of experiments, the FWHM was ≈ 2 ns at a voltage pulse amplitude of ≈ 150 kV.

* corresponding author; e-mail: VFT@loi.hcei.tsc.ru

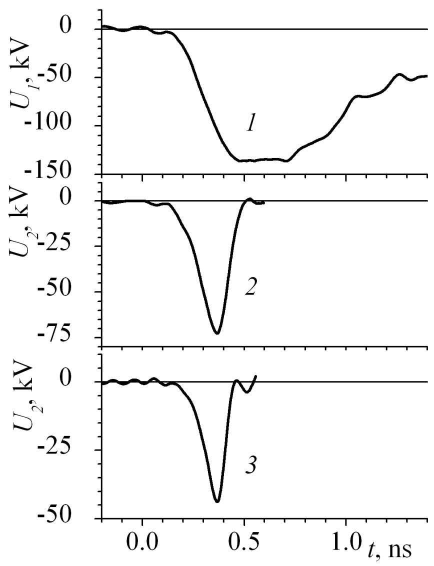

Fig. 1. Waveforms of the incident voltage wave from the capacitive dividers located at the SLEP-150 output (U_1) and in the transmission line downstream of the closing switch (U_2): incident voltage wave across the closing switch (*1*); incident voltage wave downstream of the closing switch for a gap of 3 mm (*2*) and 1 mm (*3*).

Figure 1 shows waveforms of the voltage pulses with and with no closing switch. With the closing switch, its gap was 3 and 1 mm. With a voltage pulse of FWHM ≈ 0.1 ns, the voltage risetime also approximated 0.1 ns and the voltage pulse amplitude was ≈ 45 kV (Fig. 1, curve 3). The RADAN-220 pulser had an impedance of 20 Ω. The pulser produced a voltage pulse of amplitude ≈ 250 kV (in a no load mode) and FWHM ≈ 2 ns (with a matched load) in the discharge gap at a voltage risetime of ≈ 0.5 ns. The both setups ensured a possibility to reverse the voltage polarity across the electrode of small curvature radius. The voltage pulses were measured with capacitive voltage dividers and the discharge current I was measured with the shunt composed of low-impedance chip resistors. The signals from the shunt, capacitive dividers, and collectors were recorded by TDS-6604 and DPO70604 oscilloscopes both with a 6 GHz band. Images of the integral discharge glow were taken through a grid or a window using a SONY A100 camera. The X-ray exposure dose was measured using an Arrow-Tech dosimeter (Model 138) sensitive to X-rays with a quantum energy greater than 16 keV. The dosimeter was installed 0.1–3 cm away from the foil plane and transverse to the cathode axis. The X-ray pulse shape was recorded by a diamond detector with a time resolution of ≈ 0.2 ns.

3. Experimental results and discussion

As noted above, for the ignition of an REP DD, nanosecond high-voltage pulses must be applied to the gap with an inhomogeneous electric field. The voltage pulses produced by the pulsers across the matched load had an FWHM of ≈ 2, ≈ 1, ≈ 0.2, ≈ 0.15, and ≈ 0.1 ns. However, the actual duration of the discharge current pulse was normally greater than the duration of the voltage pulse across the matched load due to the inductance of the peaking spark gap and varying impedance of the gas discharge plasma during its breakdown. Then the gas discharge chamber was filled with SF_6 at atmospheric pressure, the volume discharge was ignited. The discharge current arises during the voltage rise and its polarity does not reverse. More than 80% of the energy stored in the pulser is deposited to the discharge plasma in ≈ 3 ns. For the REP DD in SF_6, the impedance of the discharge plasma was greater than that of the pulser. In air and nitrogen as well as in inert gases, the impedance of the discharge plasma during the breakdown decreases much faster than that in SF_6, and the current of the diffuse discharge is oscillatory. The reverse of the voltage pulse polarity across the electrode of small curvature radius slightly affects the ignition of the REP DD, which agrees with the results obtained earlier [10]. The SAEB appears within 200–600 ps after the application of the voltage pulse from the pulser.

Images of the discharge glow with a negative voltage pulse across the electrode of small curvature radius for the RADAN-220 and SLEP-150 pulsers are shown in Figs. 2 and 3, respectively. Bright spots are normally evident only at the cathode. As pressure is increased, the cross-section of the discharge region with a bright glow decreases. Under these conditions, the comparatively large interelectrode gaps of the discharges in atmospheric-pressure nitrogen, air, SF_6, and other gases ensured a diffuse discharge with the longest voltage pulse durations of the pulser (≈ 2 ns at the matched load) and maximum amplitudes (≈ 250 kV). The probability of discharge constriction increased with increasing the voltage pulse duration and risetime, decreasing the interelectrode gap width, and increasing the gas pressure in the discharge chamber. Let us note that for the RADAN-220 pulser with large specific energy deposition (≈ 1 J/cm^3), constriction of the discharge occurred, and as the pressure was decreased down to tenth-hundredth of fractions of atmosphere, the REP DD to spark discharge transformation took place. The REP DD is easiest to initiate in light gases (helium, hydrogen, and neon) at high pressures. We obtained a discharge in helium with the RADAN-220 pulser at a pressure up to 15 atm.

The constriction of the discharge in air occurs earlier than that of the discharge in nitrogen. With the RADAN-220 pulser, decreasing the gap width to 4 mm ensured constriction of the atmospheric-pressure discharges in SF_6, air, and nitrogen. As the interelectrode gap width was decreased, the breakdown voltage of the discharge gap decreased, which follows from the right branch of the Paschen curve for nanosecond voltage pulse durations. For the constricted discharge, the number of oscillations per current pulse and hence the duration of the discharge current pulse increases.

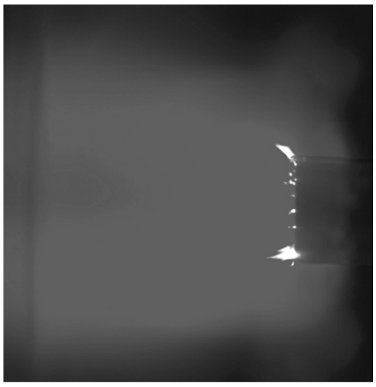

Fig. 2. Image of the discharge glow in nitrogen with an anode–cathode spacing of 14 mm. The pulser is RADAN-220, the pressure is 1 atm.

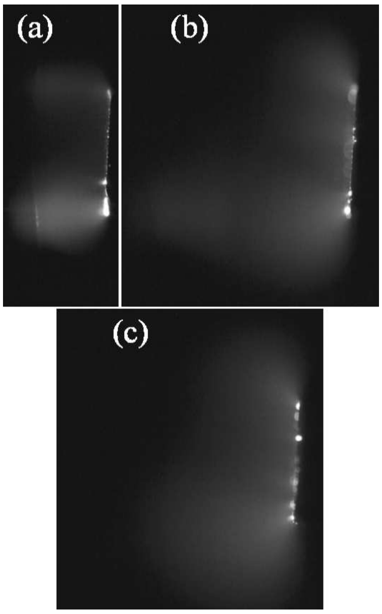

Fig. 3. Images of the discharge glow in air with an anode–cathode spacing of 4 (a), 12 (b), and 16 mm (c). The pulser is SLEP-150, the pressure is 1 atm.

Decreasing the voltage pulse duration considerably enhances the feasibility of a diffuse discharge. Figure 3 shows images of the discharge glow in air for a voltage pulse duration of ≈ 0.2 ns in the transmission line and different interelectrode gaps. Because of the decrease in voltage pulse duration, no constriction of the discharge in atmospheric pressure air was observed with a 4 mm interelectrode gap. With $d = 16$ mm, the REP DD had no time to develop and the discharge glow was observed only at the cathode, which corresponds to a pulsed corona discharge. However, cathode spots did have a chance to develop in this mode. On a pulser similar to SLEP-150, the transition to a corona discharge within ≈ 2 ns after the ignition of a diffuse discharge was observed only with a large (67 mm) interelectrode gap.

The experiments suggest that with applied voltage pulses of long duration and steep rise, the REP DD is the initial stage of a spark discharge. However, as the voltage pulse duration is increased, the diffuse stage of the REP DD, as a rule, escapes detection due to the high radiation intensity of the constricted discharge.

Figure 4 shows waveforms of the voltage pulse (incident wave 1 and wave reflected from the gap 2) and discharge current 3 with the displacement current during the voltage rise for a 12 mm gap. It is seen that with subnanosecond voltage pulses, a change in the discharge mode is observed. For a voltage pulse FWHM of < 0.2 ns (Fig. 4), the displacement current appears during the voltage rise. Under these conditions, the discharge glow corresponds to a pulsed corona discharge (Fig. 3c).

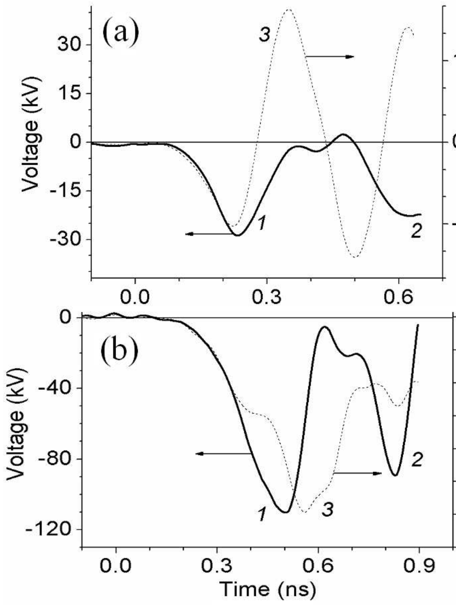

Fig. 4. Waveforms of the voltage (incident wave *1* and reflected wave *2*) and discharge current *3* with the displacement current at a voltage pulse FWHM of 0.1 ns (a) and 0.2 ns (b). The pulser is SLEP-150, the air pressure is 1 atm, the anode–cathode spacing is 12 mm.

The recording of the incident and reflected voltage waves (Fig. 4) made it possible to determine the gap voltage during the first 900 ps of the discharge development. One can distinguish two stages of the discharge: a stage before the maximum voltage across the gap and a stage after the voltage maximum. The voltage drop across the gap owes to the arrival of the dense plasma front at the anode and to the development of ionization processes in the gap. It is possible to roughly estimate the energy deposition to the gas before the gap is bridged by the ionization wave. This energy was ≈ 50 and ≈ 30 mJ for the spherical and tubular cathodes, respectively. The actual energy deposition at this discharge stage was smaller since the total input power is made up not only by the active component, but by the reactive component as well. Most of the energy is deposited to the discharge plasma once the voltage across the gap reaches its maximum, and this energy can be determined with a reasonable accuracy because the entire gap is filled with the plasma. Calculations show that once the voltage across the gap reaches its maximum, about 100 mJ is deposited to the discharge plasma within 900 ps after the beginning of the voltage pulse with both cathodes. With the tubular cathode, the time for which it was possible to determine the energy deposition was 530 ps due to the faster voltage drop across the gap and with the spherical cathode it was 350 ps. Under these conditions, the specific input power is hundreds of megawatt per cubic centimeter. The volume filled with the dense plasma is typically less than 1 cm^3 and hence the average specific power density of energy deposition in atmospheric pressure air for the tubular cathode > 200 MW/cm^3. Most of the energy ($> 90\%$) was deposited on arrival of the ionization wave front at the anode. Once the voltage across the gap reaches its maximum, the discharge mode corresponds to an anomalous pulsed glow discharge, except for one distinction. The distinction is that the current from the cathode is mainly due to explosive emission. As indicated above, almost in all gases the REP DD features bright spots at the cathode. These spots result from explosive electron emission. Let us note that in some gases, e.g., in helium and nitrogen, the REP DD can involve other mechanisms of electron emission from the cathode. In the REP DD in nitrogen, a diffuse glow with no cathode spot is observed near the side surface of the cathode (Fig. 2). Apparently, the electron emission in this cathode region is ensured by ions and photons of the VUV range.

4. Summary

The nanosecond discharge in gaps filled with nitrogen, air, and other gases in an inhomogeneous electric field was investigated. It is shown that decreasing the voltage pulse duration enhances the feasibility of a diffuse discharge with no additional ionization. The diffuse discharge is ignited due to preionization of the gap by runaway electrons and X-ray quanta. With a negative polarity of the electrode of small curvature radius, the diffuse discharge develops due to preionization by the runaway electrons resulting from electric field amplification near the cathode and in the gap with the assistance of the positive ion charge. With a positive polarity of the electrode of small curvature radius, the X-rays generated by the runaway electrons decelerated in the gap and at the anode play an important part in the ignition of the diffuse discharge. The REP DD has two characteristic stages. At the first stage, the ionization wave bridges the gap in a fraction of a nanosecond. The discharge current is determined by the conductivity of the dense plasma of the ionization wave and by the displacement current in the rest of the gap. The second discharge stage can be attributed to an anomalous glow discharge with a high specific input power. At the second stage, the voltage across the gap decreases and the cathode spots resulting from explosive electron emission can participate in the electron emission from the cathode. As the voltage pulse duration and specific input power are increased, the REP DD to spark discharge transition takes place.

The REP DD is readily realized in various gases and at different pressures. A runaway electrons preionized diffuse discharge was used for pumping different gas lasers [6], for creation VUV and UV excilamps [14–16], and for modification and cleaning of metal surfaces [17]. We suppose that REP DD will have widespread use in different fields.

Acknowledgments

This work was supported by the Russian Foundation for Basic Research (grant No. 09-08-00030-a).

References

[1] R. Noggle, E. Krider, J. Wayland, *J. Appl. Phys.* **39**, 4746 (1968).

[2] L. Tarasova, L. Khudyakova, *J. Tech. Phys.* **39**, 1530 (1969).

[3] L. Babich, T. Lojko, *J. Tech. Phys.* **61**, 153 (1991).

[4] L. Tarasova, L. Khudyakova, T. Loiko, V. Tsukerman, *J. Tech. Phys.* **44**, 564 (1974).

[5] V. Tarasenko, V. Orlovskii, S. Shunailov, *Russian Phys. J.* **46**, 325 (2003).

[6] S. Alekseev, V. Gubanov, I. Kostyrya, V. Orlovskii, V. Tarasenko, *Quantum Electron.* **34**, 1007 (2004).

[7] I. Kostyrya, V. Orlovskii, V. Tarasenko, A. Tkachev, S. Yakovlenko, *Tech. Phys. Lett.* **31**, 457 (2005).

[8] P. Repin, A. Rep'ev, *Tech. Phys.* **53**, 73 (2008).

[9] V. Tarasenko, *Appl. Phys. Lett.* **88**, 081501 (2006).

[10] V. Tarasenko, E. Baksht, A. Burachenko, I. Kostyrya, M. Lomaev, D. Rybka, *Plasma Devices Operation* **16**, 267 (2008).

[11] V. Tarasenko, D. Rybka, E. Baksht, I. Kostyrya, M. Lomaev, *Instrum. Exp. Techn.* **51**, 213 (2008).

[12] V. Tarasenko, E. Baksht, A. Burachenko, I. Kostyrya, M. Lomaev, D. Rybka, *Laser Particle Beams* **26**, 605 (2008).

[13] V. Tarasenko, E. Baksht, A. Burachenko, I. Kostyrya, M. Lomaev, D. Rybka, *IEEE Trans. Plasma Sci.* **37**, 832 (2009).

[14] E. Baksht, D. Rybka, M. Lomaev, V. Tarasenko, *Quantum Electron.* **36**, 576 (2006).

[15] M. Lomaev, G. Mesyats, D. Rybka, V. Tarasenko, E. Baksht, *Quantum Electron.* **37**, 595 (2007).

[16] M. Erofeev, V. Tarasenko, *Quantum Electron.* **38**, 401 (2008).

[17] M. Shulepov, V. Tarasenko, I. Goncharenko, N. Koval', I. Kostyrya, *Tech. Phys. Lett.* **34**, 296 (2008).